13th European Conference on Composite Materials, June 2 - 5, 2008, Stockholm, Sweden

A SIMPLIFIED DISCRETE FINITE ELEMENT MODEL FOR NON-CRIMP FABRIC COMPOSITES

Christian Knipprath[1], Alexandros A. Skordos[1] and Anthony K. Pickett[2]

[1]Composites Centre, School of Applied Sciences, Cranfield University, MK43 0AL Cranfield, UK
[2]IFB, Institute for Aircraft Design, University of Stuttgart, Germany

ABSTRACT

In this paper a simplified discrete finite element model for composite materials is introduced. This model allows the discrete representation of both the fibre tows and the resin on a meso-scale level. The capability to assign different material properties to each fibre tow and resin zones allows the investigation of local reinforcements in composites. This modelling concept is combined with a three dimensional damage model and is successfully implemented in a finite element code. Results indicate that relatively fast model analysis and successful approximation of fibre and resin failure under specific load cases may be investigated.

1. INTRODUCTION

The simulation of mechanical behaviour of composite materials is based on two types of approaches: (i) continuum models in which homogenised material properties are used [1, 2]; and (ii) discrete models in which resin and fibre tows are represented as separate materials [3, 4]. Continuum models are computationally efficient and thus appropriate for modelling the mechanical response of relatively large structures, whereas discrete models operate at the meso-level and offer greater predictive capabilities at the cost of solution time.

This paper introduces a simplified method for the modelling of tow based composite materials which allows the discrete representation of matrix and fibre tows. The methodology proposed here is based on concepts originally developed for modelling the draping of non-crimp fabrics [5] and constitutes an intermediate solution that combines relative computational efficiency with the capability to model fibre tows and resin separately. This type of representation allows easy incorporation of the influence of local reinforcements with respect to both variations in material properties and local tow architecture.

The modelling methodology is combined with a three dimensional damage model based on the concepts originally presented in [2, 6]. The model represents the reduction of material properties due to failure via damage parameters. Three characteristic damage modes for composites are included in this type of treatment: (i) matrix micro-cracking, (ii) fibre/matrix debonding and (iii) fibre rupture. The composite damage model implemented here follows the same approach. Under the assumption of a three-dimensional stress-state, damage parameters are introduced for each material direction respectively. This leads to an extended representation of the material behaviour so that damage is introduced and can evolve independently for each material direction.

2. MODEL METHODOLOGY

The finite element model represents the fibre tows and the resin separately within a Non-Crimped Fabric (NCF) composite using 3-d elements for tows and cohesive

interface for the resin. An idealisation of the model is illustrated in Figures 1.a and 1.b. The shape of tows is simplified in order to allow the use of a limited number of hexahedral elements whereas the resulting gaps between the idealised fibre tows are used to embody the resin zones with cohesive elements to simulate the initiation and the progress of delamination.

The stress components of a cohesive element are expressed via the local coordinate system while the related deformations are calculated using the relative displacements between the element top and bottom faces. The fibre tows are represented with solid elements and share the same nodes with the cohesive elements as shown in Figure 1.c.

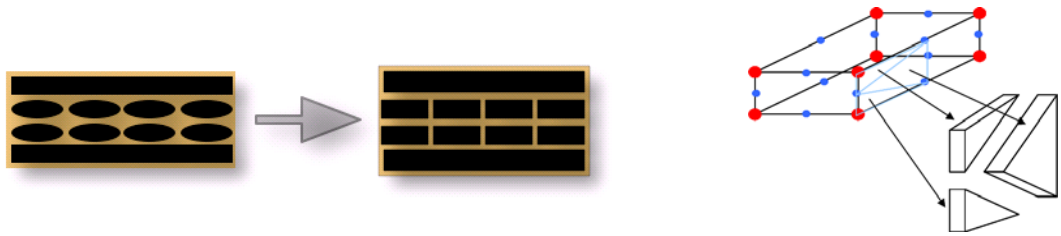

a) b) c)

Figure 1: Model concept: a) NCF composite tow-level architecture; b) simplified architecture and; c) finite element discretisation.

This approach allows the investigation of the influence of local variations of material properties on the mechanical performance of NCF composites. Different material properties can be assigned to the corresponding elements which allows reasonable stress distributions to be predicted in the model at the meso-scale.

3. MATERIAL DAMAGE MODEL

The composite damage model introduced in the following section follows the same approach reported in [2, 6-8]. Damage parameters for each direction are introduced under the assumption of a three-dimensional stress state. These parameters represent the accumulated damage state in different directions.

3.1. DAMAGE KINEMATICS OF THE FIBRE TOW

3.1.1. MODEL FORMULATION

Under the assumption of a three-dimensional stress state the elastic volumetric energy for a composite material can be expressed in the following form:

$$W_e = \frac{1}{2}\left[\frac{{\sigma_{11}}^2}{E_{11}} + \frac{{\sigma_{22}}^2}{E_{22}} + \frac{{\sigma_{33}}^2}{E_{33}} - \left(\frac{\nu_{12}}{E_{11}} + \frac{\nu_{21}}{E_{22}}\right)\sigma_{11}\sigma_{22} - \left(\frac{\nu_{13}}{E_{11}} + \frac{\nu_{31}}{E_{33}}\right)\sigma_{11}\sigma_{33} - \left(\frac{\nu_{23}}{E_{22}} + \frac{\nu_{32}}{E_{33}}\right)\sigma_{22}\sigma_{33} + \frac{{\sigma_{12}}^2}{G_{12}} + \frac{{\sigma_{13}}^2}{G_{13}} + \frac{{\sigma_{23}}^2}{G_{23}}\right]. \quad (1)$$

From this energy expression the elastic strain tensor is derived using the relation

$$\varepsilon_{ij}^{\ e} = \frac{\partial W_e}{\partial \sigma_{ij}} \quad . \quad (2)$$

By reassembling these expressions and changing from tensor to vector notation it is possible to derive the stress vector components. With further rearrangements the entries for the orthotropic elasticity matrix are obtained, in which each component depends on the material parameters E_{kl} and ν_{kl}.

3.1.2. DAMAGE PARAMETERS

Scalar damage factors are introduced in each direction to simulate the reduction of stiffness. Damage parameters can be augmented in a damage parameter vector $\overline{d}$ as follows,

$$\overline{d} = \left(d_2, d_3, d_{12}, d_{23}, d_{13} \right)^T \quad . \tag{3}$$

The damage parameters are independently calculated from a set of thermodynamic variables for each direction and represent the energy dissipation due to damage. The damage factor in the fibre direction d_{11} is calculated separately as shown below.

3.1.3. BEHAVIOUR IN FIBRE DIRECTION

The behaviour in the fibre direction is dominated by a semi-brittle response. Experiments show brittle linear elastic behaviour in tension and a non-linear elastic behaviour in compression [8]. The compressive stiffness loss is expressed as follows,

$$E_{11}{}^{\gamma} = \frac{E_{11}^{0c}}{1 + \gamma E_{11}^{0c} \, | \varepsilon_{11} |} \quad . \tag{4}$$

Here E_{11}^{0c} is the initial compressive modulus and γ a material constant. Three different stages in the development of damage can be assumed. Figure 2 illustrates the fibre behaviour for tension and compression.

Tension $\sigma_{11} \geq 0$:

$$\begin{array}{lllll}
\text{pre-critical} & E_{11}{}^{t} = E_{11}{}^{0t} & & \text{for} & \varepsilon_{11} \leq \varepsilon_i{}^{t} \\
\text{critical} & E_{11}{}^{t} = (1 - d_1{}^{t}) E_{11}{}^{0t} & d_1{}^{t} = d_u{}^{t} \dfrac{\varepsilon_{11} - \varepsilon_i{}^{t}}{\varepsilon_u{}^{t} - \varepsilon_i{}^{t}} & \text{for} & \varepsilon_i{}^{t} < \varepsilon_{11} \leq \varepsilon_u{}^{t} \\
\text{post-critical} & E_{11}{}^{t} = (1 - d_1{}^{t}) E_{11}{}^{0t} & d_1{}^{t} = 1 - (1 - d_u{}^{t}) \dfrac{\varepsilon_u{}^{t}}{\varepsilon_{11}} & \text{for} & \varepsilon_u{}^{t} < \varepsilon_{11} \leq \infty
\end{array} \tag{5}$$

Compression $\sigma_{11} < 0$:

$$\begin{array}{lllll}
\text{pre-critical} & E_{11}{}^{c} = E_{11}{}^{\gamma} & & \text{for} & | \varepsilon_{11} | \leq \varepsilon_i{}^{c} \\
\text{critical} & E_{11}{}^{c} = (1 - d_1{}^{c}) E_{11}{}^{\gamma} & d_1{}^{c} = d_u{}^{c} \dfrac{| \varepsilon_{11} | - \varepsilon_i{}^{c}}{\varepsilon_u{}^{c} - \varepsilon_i{}^{c}} & \text{for} & \varepsilon_i{}^{c} < | \varepsilon_{11} | \leq \varepsilon_u{}^{c} \\
\text{post-critical} & E_{11}{}^{c} = (1 - d_1{}^{c}) E_{11}{}^{\gamma} & d_1{}^{c} = 1 - (1 - d_u{}^{c}) \dfrac{\varepsilon_u{}^{c}}{| \varepsilon_{11} |} & \text{for} & \varepsilon_u{}^{c} < | \varepsilon_{11} | \leq \infty
\end{array} \tag{6}$$

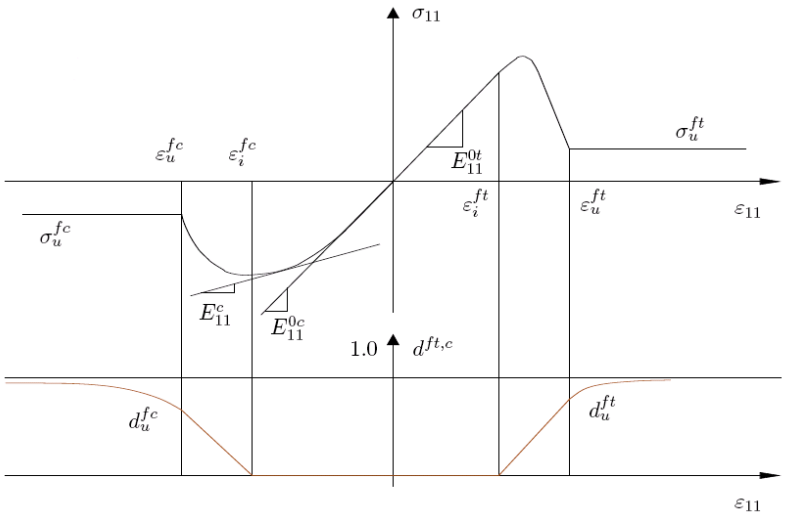

Figure 2: Fibre behaviour under tension and compression loading [9].

3.1.4 INFLUENCE OF DAMAGE IN THE OTHER DIRECTIONS

In transverse direction micro-cracks appear due to tensile loading. It is assumed that these cracks will close under compression and consequently have no damaging effect in compression [5]. The moduli are therefore calculated as follows

- Transverse direction:

$$\begin{aligned}
&\text{tension:} && E_{22} = (1-d_2)E_{22}^{\ 0} && \text{if} && \varepsilon_{22} + \nu_{12}\varepsilon_{11} + \nu_{32}\varepsilon_{33} > 0 \\
&\text{compression:} && E_{22} = E_{22}^{\ 0} && \text{if} && \varepsilon_{22} + \nu_{12}\varepsilon_{11} + \nu_{32}\varepsilon_{33} \le 0 \\
&\text{tension:} && E_{33} = (1-d_3)E_{33}^{\ 0} && \text{if} && \varepsilon_{33} + \nu_{13}\varepsilon_{11} + \nu_{23}\varepsilon_{22} > 0 \\
&\text{compression:} && E_{33} = E_{33}^{\ 0} && \text{if} && \varepsilon_{33} + \nu_{13}\varepsilon_{11} + \nu_{23}\varepsilon_{22} \le 0
\end{aligned} \tag{7}$$

- Shear direction:

$$\begin{aligned}
G_{12} &= (1-d_{12})G_{12}^{\ 0} \\
G_{23} &= (1-d_{23})G_{23}^{\ 0} \\
G_{13} &= (1-d_{13})G_{13}^{\ 0}
\end{aligned} \tag{8}$$

3.1.5. CALCULATION OF THE DAMAGE PARAMETERS

A set of thermodynamic quantities Z_i is used to describe the dissipation associated with the damage variables. These values are calculated as follows,

$$Z_i = \frac{\partial W_e}{\partial d_i} \tag{9}$$

Damage evolution is governed by these variables in the same manner as the energy release rate describes crack propagation due to delamination in a composite [10]. With the aid of these expressions another set of variables is derived to describe matrix micro-cracking and fibre/matrix debonding

$$\overline{Y} = \begin{cases} Y_2(t) = \overset{\max}{\tau \le t}\left[\sqrt{Z_2(\tau) + a_1 Z_{12}(\tau) + a_2 Z_{23}(\tau)}\right] \\ Y_3(t) = \overset{\max}{\tau \le t}\left[\sqrt{Z_3(\tau) + a_3 Z_{13}(\tau) + a_4 Z_{23}(\tau)}\right] \\ Y_{12}(t) = \overset{\max}{\tau \le t}\left[\sqrt{Z_{12}(\tau) + b_1 Z_2(\tau)}\right] \\ Y_{13}(t) = \overset{\max}{\tau \le t}\left[\sqrt{Z_{13}(\tau) + b_2 Z_3(\tau)}\right] \\ Y_{23}(t) = \overset{\max}{\tau \le t}\left[\sqrt{Z_{23}(\tau) + b_3 Z_3(\tau)}\right] \end{cases} . \tag{10}$$

These variables act as thresholds and define the undamaged region. Here a_i and b_i are coupling factors. The evolution for each damage factor follows the same procedure. In the case of d_2 the evolution can be expressed as follows:

$$\begin{aligned} &\text{if} \quad d_2 < d_{2max} \quad \& \quad Y_2(t) < Y_2 \quad \& \quad Y_{12}(t) < Y_{12R} \\ &\qquad d_2 = \frac{\left\langle Y_2(t) - Y_{2,0} \right\rangle_+}{Y_{2,c}} \\ &\text{else} \quad d_2 = d_{2max} \end{aligned} \tag{11}$$

The damage depends on the values $Y_2, Y_{12R}, Y_{2,0}$ and $Y_{2,c}$. These threshold values correspond to brittle transverse damage of the fibre/matrix interface, shear fracture, initial shear damage and critical shear damage respectively.

3.1.6. MODELLING OF INELASTIC STRAINS

An extended version of the plastic model introduced in [2] is used for NCF composites. It is a von Mises yield criterion that uses an associated flow rule to follow the permanent plastic strains in the matrix.

$$f(\sigma, \overline{\varepsilon}^p) = \sqrt{(\sigma_{22}{}^2 + \sigma_{33}{}^2)c^2 + \sigma_{12}{}^2 + \sigma_{13}{}^2 + \sigma_{23}{}^2} - R(\overline{\varepsilon}^p) \tag{12}$$

It is assumed that the stress component σ_{11} has no contribution on plasticity development. Factor c^2 accounts for material anisotropy whilst plastic strain hardening is assumed to follow a power law

$$R(\overline{\varepsilon}^p) = R_0 + \beta(\overline{\varepsilon}^p)^m \quad . \tag{13}$$

Where R_0 is the initial shear yield stress, and β and m are curve fitting parameters; $\overline{\varepsilon}^p$ is the equivalent plastic strain.

4. SIMULATION OF DIFFERENT LOAD CASES

Three simulations with different load cases were carried out to evaluate the capabilities of the proposed modeling technique using MSC.Marc as the solver [10]. A unidirectional (UD) NCF composite panel with the dimensions 20 x 20 x 4 mm is used

for the following simulations: (i) bending; (ii) tension in the fibre direction; and (iii) an impact scenario. The necessary material data was taken from [11, 12] and are summarised in Table 1.

	Notation	Symbol	Value
Mechanical properties	Fibre tension modulus	E_{11}^{t0}	114 GPa
	Fibre compression modulus	E_{11}^{c0}	80 GPa
	Matrix transverse modules	E_{22}^{0}	7.8 GPa
		E_{33}^{0}	7.8 GPa
	Matrix shear modules	G_{12}^{0}	2.85 GPa
		G_{13}^{0}	2.85 GPa
		G_{23}^{0}	2.5 GPa
	Poisson's ratios	ν_{12}	0.32
		ν_{23}	0.4
		ν_{31}	0.03
	Matrix yield stress	R_0	0.02 GPa
	Matrix hardening coefficient	β	0.67 GPa
	Matrix hardening exponent	m	0.52
	Mode I energy release rate	G_{Ic}	470 J/m^2
	Critical opening displacement	v_c	1.923 μm
	Shear/normal weighting coefficient	G_{IIc}/G_{Ic}	4.255
Damage properties	Max. tensile and compressive fibre damage value	d_u^t	0.96
		d_u^c	0.96
	Initial and ultimate tensile fibre damage strain	ε_i^t	0.015
		ε_u^t	0.02
	Initial and ultimate compressive fibre damage strain	ε_i^c	0.0175
		ε_u^c	0.02
	Brittle transverse damage threshold of fibre/matrix interface	Y_{2S}	24.3 $\sqrt{GPa}$
		Y_{3S}	24.3 $\sqrt{GPa}$
	Elementary shear damage threshold	Y_{12R}	42 $\sqrt{GPa}$
		Y_{13R}	42 $\sqrt{GPa}$
		Y_{23R}	31 $\sqrt{GPa}$ *
	Initial transverse damage threshold	$Y_{12,0}$	0.949 $\sqrt{GPa}$
		$Y_{13,0}$	0.949 $\sqrt{GPa}$
		$Y_{23,0}$	0.732 $\sqrt{GPa}$ *
	Critical transverse damage threshold	$Y_{12,c}$	189.7 $\sqrt{GPa}$
		$Y_{13,c}$	189.7 $\sqrt{GPa}$
		$Y_{23,c}$	109.6 $\sqrt{GPa}$ *
	Initial shear damage threshold	$Y_{2,0}$	0.632 $\sqrt{GPa}$

Critical shear damage threshold	$Y_{3,0}$	$0.632\sqrt{GPa}$
	$Y_{2,c}$	$107.5\sqrt{GPa}$
	$Y_{3,c}$	$107.5\sqrt{GPa}$

Table 1: Summary of the material model parameters [11, 12]; * estimated values

4.1 PANEL BENDING SIMULATION

The first simulation covers a bending scenario with a pre-described displacement in the thickness direction reaching a maximum displacement of 10 mm. Figure 3.a shows the applied boundary conditions. Delamination failure of the resin occurs near to the constrained panel edge in the inter-tow region as shown in Figure 3.b where the bending moment reaches its maximum value.

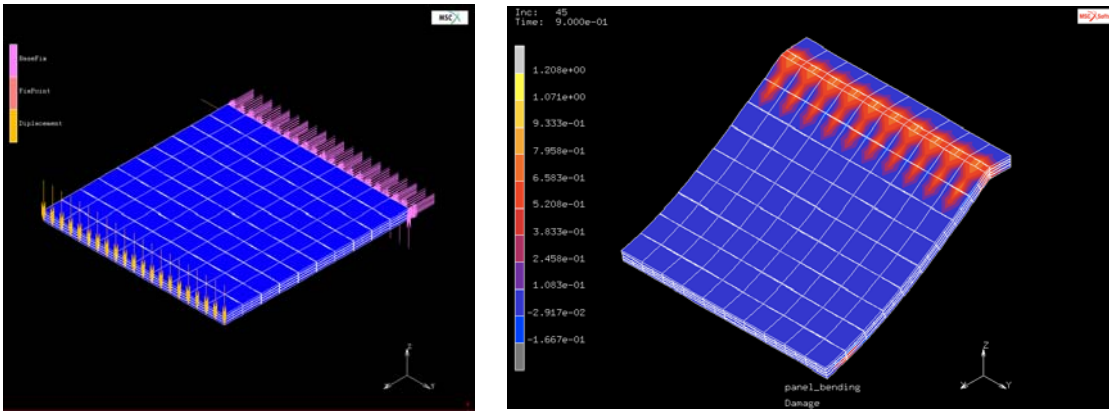

a) b)

Figure 3: Bending simulation: a) NCF composite panel with the applied boundary conditions/load; and b) damage at the end of the simulation.

4.2 PANEL UNDER TENSION

In the next load case the panel is fixed on one side and a pre-scribed displacement is applied to the other edge as shown in Figure 4.a. Maximum displacement is set to 0.44 mm. Figure 4.b illustrates the reaction force for the final stage of the simulation. At this simulation time the stiffness of the elements in the fibre direction are reduced to a minimum value. As a consequence the fibres do not carry further significant load.

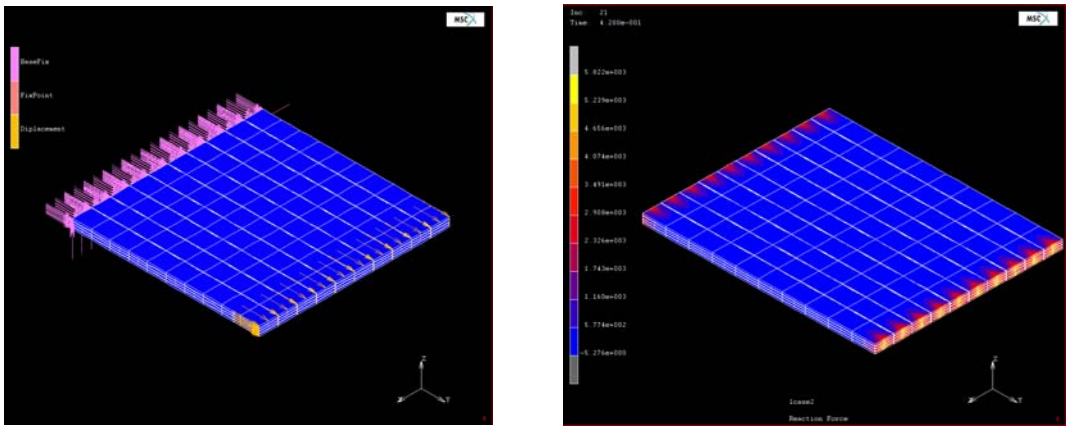

a) b)

Figure 4: NCF panel under tension: a) boundary conditions and load case; and b) reaction force of the fibres in [N].

Figure 5 illustrates the stress displacement curve for Node 12100 located nearby the displacement applied edge. The peak reaches a maximum value of 1.51 GPa before the fibre degradation due to damage starts and drops after exceeding the initial tensile

strain ε_i^t as described in section 3.1.3. Thereafter a constant minimal stress level remains once the ultimate tensile strain ε_u^t is reached to prevent numerical instability problems.

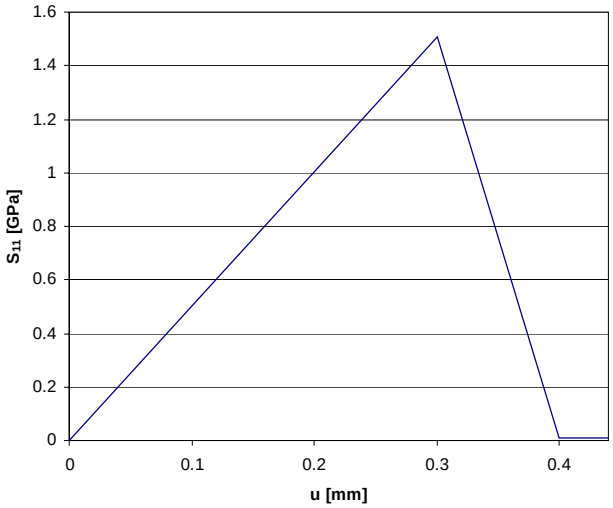

Figure 5: Stress-displacement curve at a node in the prescribed displacement side.

4.3 IMPACT SCENARIO

Figure 6.a illustrates the setup for the impact scenario. The approaching velocity of the impactor is set to 3.464 m/s with a total mass of 5 kg, giving an impact energy of 30 J. The displacement map in the thickness direction is shown in Figure 6.b.

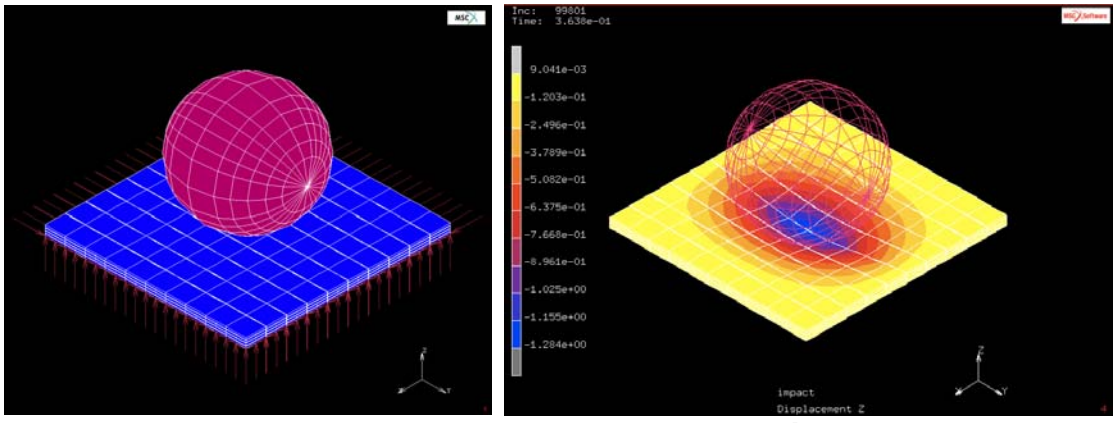

a) b)

Figure 6: Impact simulation: a) boundary conditions and approaching impactor; b) displacement in Z-direction due to the applied load.

Figure 7 illustrates the damaged matrix regions of the panel at the end of the simulation from top and bottom perspective. The main damage occurs in the direct impact zone although a significant influence can be seen in the surrounding area. The zones highlighted in yellow represent the damage due to tension while the blue zones indicate compressive damage.

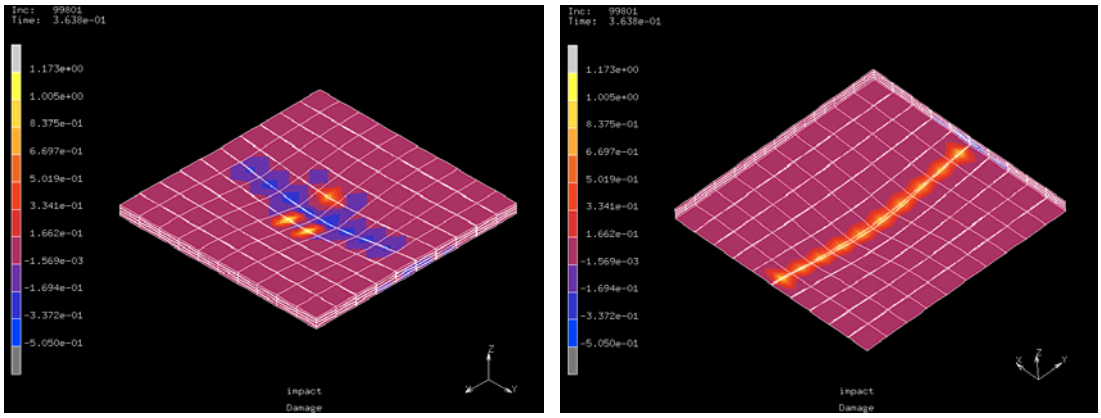

a) b)

Figure 7: Damage map: a) view from above; b) view from below

5. CONCLUDING REMARKS

The results of finite element model indicated satisfactory performance combined with good approximation of fibre and resin dominated damage. The current version of the model handles the damage in the fibre direction and in the transverse and shear directions with different approaches which leads to an inconvenient numerical implementation. A consistent approach has been proposed [13] which derives the fibre damage from the energy dissipation of the material, in the same way as for the matrix components. According to this procedure the fibre stress component can be incorporated in the yield stress calculation. A recently introduced yield criterion for concrete [14] offers great potential for the representation of composite material behaviour. This criterion, which is illustrated in Figure 8, is capable of including the brittle material behaviour in the fibre direction by locally extending the von Mises yield surface. This approach will form the basis of further development of the simplified model developed here.

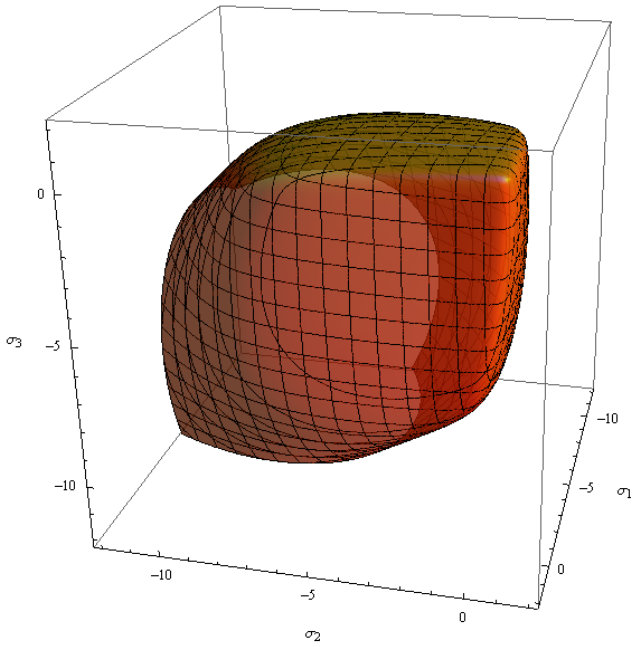

Figure 8: Yield criterion for concrete [14].

ACKNOWLEDGEMENTS

Financial support from the CEC under the PreCarBi project (FP6-30848) is gratefully acknowledged

REFERENCES

1- Allen, D.H., "Homogenization principles and their application to continuum damage mechanics.", *Composites Science and Technology*, (2001),61: 2223–2230.
2- Ladevèze, P. and LeDantec, E., "Damage Modelling of the Elementary Ply for Laminated Composites.", *Composites Science and Technology(UK)* , (1992), 43: 257-267.
3- Edgren et al., "Formation of damage and its effects on non-crimp fabric reinforced composites loaded in tension.", *Composites Science and Technology*, (2004),64: 675–692.
4- Edgren et al., "Failure of NCF composites subjected to combined compression and shear loading.", *Composites Science and Technology*, (2006),66: 2865–2877.
5- Creech, G. and Pickett, A.K., "Meso-modelling of Non-Crimp Fabric composites for coupled drape and failure analysis.", *Journal of Materials Science*, (2006),41: 6725–6736.
6- Ladevèze, P. et al., "A mesomodel for localisation and damage computation in laminates.", *Computer Methods in Applied Mechanics and Engineering*, (2000), 183: 105-122.
7- Allix, O. and Ladevèze, P., "Interlaminar Interface Modelling for the Prediction of Delamination.", *Composite Structures(UK)*, (1992),22: 235-242.
8- Allix, O. et al., "Modelling and Identification of the Mechanical Behaviour of Composite Laminates in Compression.", *Composites Science and Technology (UK)*, (1994), 51:35-42.
9- PAM-CRASH^{TM} Version 2002 Manual, PAM System International

10- MSC Software Corporation, “MSC.Marc User Manual”, (2005)
11- Greve, L. and Pickett, A.K., “Modelling damage and failure in carbon/epoxy non-crimp fabric composites including effects of fabric pre-shear.”, *Composites Part A*, (2006), 37: 1983-2001.
12- Greve, L. and Pickett, A.K., “Delamination testing and modelling for composite crash simulation.”, *Composites Science and Technology*, (2006),66: 816–826.
13- Allix, O., “A composite damage meso-model for impact problems.”, *Composites Science and Technology*, (2001),61: 2193–2205.
14- Francois, M., “A new yield criterion for the concrete materials.”, *Comptes Rendus Mécanique* , in press., Available online 4 March 2008.